Porath, J., & Larsson, B. (1978) *J. Chromatogr. 155*, 47–68.
Puca, G. A., Nola, E., Sica, V., & Bresciani, F. (1972) *Biochemistry 11*, 4157–4165.
Redeuilh, G., Secco, C., Baulieu, E.-E., & Richard-Foy, H. (1981) *J. Biol. Chem. 256*, 11496–11502.
Sakai, D., & Gorski, J. (1984) *Endocrinology (Baltimore) 115*, 2379–2383.
Sawyer, W. H., & Puckridge, J. (1973) *J. Biol. Chem. 248*, 8429–8433.
Scatchard, G. (1949) *Ann. N.Y. Acad. Sci. 51*, 660–672.
Sherman, M. R., & Stevens, J. (1984) *Annu. Rev. Physiol. 46*, 83–105.
Sherman, M. R., Tuazon, F. B., & Miller, L. K. (1980) *Endocrinology (Baltimore) 106*, 1715–1727.
Sherman, M. R., Tuazon, F. B., Stevens, Y.-W., & Niu, E. M. (1983) in *Steroid Hormone Receptors: Structure and Function* (Eriksson, H., & Gustafsson, J.-A., Eds.) pp 3–24, Elsevier, Amsterdam.
Sherman, M. R., Stevens, Y.-W., & Tuazon, F. B. (1984) *Cancer Res. 44*, 3783–3796.
Sluyterman, L. A. AE., & Elgersma, O. (1978) *J. Chromatogr. 150*, 17–30.
Sluyterman, L. A. AE., & Wijdenes, J. (1978) *J. Chromatogr. 150*, 31–44.
Stark, G. R., Stein, W. H., & Moore, S. (1960) *J. Biol. Chem. 235*, 3177–3181.

Homology-Dependent Changes in Adenosine 5′-Triphosphate Hydrolysis during *recA* Protein Promoted DNA Strand Exchange: Evidence for Long Paranemic Complexes†

Brian C. Schutte and Michael M. Cox*
Department of Biochemistry, College of Agriculture and Life Sciences, University of Wisconsin—Madison, Madison, Wisconsin 53706

Received December 5, 1986; Revised Manuscript Received April 20, 1987

ABSTRACT: As a first step in DNA strand exchange, *recA* protein forms a filamentous complex on single-stranded DNA (ssDNA), which contains stoichiometric (one *recA* monomer per four nucleotides) amounts of *recA* protein. *recA* protein monomers within this complex hydrolyze ATP with a turnover number of 25 min^{-1}. Upon introduction of linear homologous duplex DNA to initiate strand exchange, this rate of ATP hydrolysis drops by 33%. The decrease in rate is complete in less than 2 min, and the rate of ATP hydrolysis then remains constant during and subsequent to the strand exchange reaction. This drop is completely dependent upon homology in the duplex DNA. In addition, the magnitude of the drop is linearly dependent upon the *length* of the homologous region in the linear duplex DNA. Linear DNA substrates in which pairing is topologically restricted to a paranemic joint also follow this relationship. Taken together, these properties imply that all of the available homology in the incoming duplex DNA is detected very early in the DNA strand exchange reaction, with the linear duplex DNA paired *paranemically* with the homologous ssDNA in the complex throughout its length. The results indicate that paranemic joints can extend over thousands of base pairs. We note elsewhere [Pugh, B. F., & Cox, M. M. (1987b) *J. Biol. Chem. 262*, 1337–1343] that this duplex acquires resistance to digestion by DNase with a much slower time course (30 min), which parallels the progress of strand exchange. Together these results imply that the duplex DNA is paired with the ssDNA but remains outside the nucleoprotein filament. Finally, the results also support the notion that ATP hydrolysis occurs throughout the *recA* nucleoprotein filament.

The *recA* protein of *Escherichia coli* promotes a series of in vitro DNA strand exchange reactions that mimic its in vivo function in homologous genetic recombination (DasGupta et al., 1980; Cox & Lehman, 1981a). The best characterized of these reactions is a three-strand exchange in which the *recA* protein promotes the exchange of complementary strands between linear duplex and circular single-stranded DNA molecules derived from bacteriophages. The products of this reaction are a nicked circular heteroduplex DNA and the displaced linear single-stranded DNA (ssDNA).[1] The reaction can be divided into three experimentally distinguishable phases. The first is presynapsis, the cooperative binding of stoichiometric amounts of *recA* protein to ssDNA in the presence of ATP (Cox & Lehman, 1982; Radding et al., 1983; Flory et al., 1984; Morrical et al., 1986). This complex exhibits a stoichiometry of one *recA* monomer per four nucleotides (Cox & Lehman, 1987) and exhibits a filamentous structure in the electron microscope (Flory & Radding, 1982; Dunn et al., 1982). The second phase is synapsis, the search for homology and eventual alignment of the duplex DNA with homologous sequences on the ssDNA (Shibata et al., 1979;

† This work was supported by National Institutes of Health Grant GM32335. B.C.S. was supported by Training Grant GM07215 from the National Institutes of Health. M.M.C. is supported by National Institutes of Health Research Career Development Award AI00599.
* Author to whom correspondence should be addressed.

[1] Abbreviations: ssDNA, single-stranded DNA; dsDNA, double-stranded DNA; M13mp8(+), circular single-stranded genome of bacteriophage M13mp8; Tris, tris(hydroxymethyl)aminomethane; EDTA, ethylenediaminetetraacetic acid; DTT, dithiothreitol; bp, base pair(s); SSB, *Escherichia coli* single-stranded DNA binding protein; SDS, sodium dodecyl sulfate.

0006-2960/87/0426-5616$01.50/0 © 1987 American Chemical Society

McEntee et al., 1979; Cox & Lehman, 1981a; DasGupta & Radding, 1982). If a free end is available at the site of this pairing, a nascent heteroduplex joint is formed (Wu et al., 1982; Kahn & Radding, 1984). The final phase is branch migration, the unidirectional extension of this heteroduplex, coupled to the hydrolysis of ATP (Cox & Lehman, 1981a,b; Kahn et al., 1981; West et al., 1981).

For purposes of this paper, several aspects of the second and third phases of this reaction require elaboration. The alignment of homologous sequences of two DNA molecules in the second phase can involve two different types of homologous synapse, as identified in work initiated by Radding and colleagues (DasGupta et al., 1980; Cunningham et al., 1981; Bianchi et al., 1983). The first of these is a paranemic joint. In this case the DNA molecules are homologously aligned, but there is no extended crossover interwinding or base pairing (in the Watson–Crick sense) involving complementary strands derived from each DNA. The two DNA molecules can readily be separated without topological restriction. A plectonemic joint is defined by the presence of strand crossover, with interwinding and base pairing over a short region. Recently, these terms were defined operationally by their lack of stability (paranemic) or stability (plectonemic) in the presence of protein denaturants (Riddles & Lehman, 1985). Formation of a homologous synapse through a paranemic joint can be demonstrated by employing homologous substrates that do not contain a free end at a site of homology (DasGupta et al., 1980; Bianchi et al., 1983; Riddles & Lehman, 1985). Thus, crossover strand interwinding is topologically restricted. These complexes are easily disrupted, and no information is available about their structure. We note only one suggestion in the literature to date (Howard-Flanders et al., 1984).

Several attempts have been made to estimate the size of the region paired in the initial paranemic complex. Kinetic methods revealed rapid formation of a short 100–300-bp region of heteroduplex DNA early in strand exchange (Wu et al., 1982; Kahn & Radding, 1984). Since the assays used in these experiments were designed to detect interwound heteroduplex DNA, no direct information about the size of paranemic joints was obtained. Wu et al. (1983) observed unwinding of 1000 bp or more of the duplex DNA, which was clearly associated with the formation of paranemic complexes. This unwinding, however, occurred over 10–30 min. The effect was therefore not kinetically competent to reflect an event in the normal synapsis pathway. Paranemic joints have been observed directly by electron microscopy, which exhibited a length of 300–400 bp (Christiansen & Griffith, 1986). The length of these joints, however, was subject to topological limitations imposed by the supercoiled duplex DNA employed in the experiments, and the size estimate must be considered a minimum. No information is available in the literature concerning the upper limit for the length of a paranemic complex. Whatever their size, paranemic joints are intermediates in the formation of the second type of homologous synapse, the plectonemic joint (Bianchi et al., 1983; Riddles & Lehman, 1985). The plectonemic joint forms the starting point for the third phase of strand exchange.

We are especially interested in this final phase of the reaction. The coupling of ATP hydrolysis to unidirectional branch migration represents a coupled vectorial system analogous in a sense to muscle contraction and ATP-driven ion pumps. The active species in this reaction is a nucleoprotein filament of *recA* protein and ssDNA. A current goal is to define a model for this reaction that provides a role for the nucleoprotein filament and also explains a host of other observations. This task requires detailed information about the location of *recA* protein and each DNA strand at all stages of the reaction, as well as the role of ATP hydrolysis in the reaction.

In order to investigate the role of ATP in this reaction, we have undertaken a study of rates of ATP hydrolysis during strand exchange. The rates have been found to be constant throughout the reaction, with the exception of a 33% drop in the rate of ATP hydrolysis which occurs immediately after the introduction of the homologous duplex DNA substrate. We do not know the molecular basis for this decrease. The properties of this effect, however, provide strong evidence that early in the reaction the duplex and single-stranded DNA molecules are paired paranemically throughout their homologous length; i.e., the paranemic joint initially described by Radding and colleagues can extend over thousands of base pairs. When combined with other evidence, a proposed structure for this paranemic complex emerges that has important structural and energetic implications for the mechanism of DNA strand exchange. We also demonstrate that ATP hydrolysis cannot be divided into ssDNA- and dsDNA-dependent components during strand exchange as suggested by Roman and Kowalczykowski (1986).

Materials and Methods

Enzymes and DNA. *E. coli recA* protein was purified and stored as previously described (Cox et al., 1981). The concentration of *recA* protein in stock solutions was determined by the absorbance at 280 nm, with an extinction coefficient of $\epsilon_{280} = 0.59\ A_{280}\ mg^{-1}\ mL$ (Craig & Roberts, 1981). *E. coli* SSB protein was purified by the method of Lohman et al. (1986) and was stored frozen at −70 °C in a buffer containing 20 mM Tris, 40% cation (pH 8.4), 0.15 M NaCl, 1 mM EDTA, 1 mM β-mercaptoethanol, and 50% glycerol. The concentration of SSB protein stock solutions was determined by the absorbance at 280 nm, with an extinction coefficient of $\epsilon_{280} = 1.5\ A_{280}\ mg^{-1}\ mL$ (Lohman & Overman, 1985). Single-stranded DNA derived from bacteriophage M13mp8 was prepared as described (Messing, 1983). Circular duplex DNA derived from the bacteriophages M13oriC26 (Kaguni et al., 1979) and M13mp8, as well as plasmid DNA, was prepared as described (Neuendorf & Cox, 1986; Messing, 1983; Davis et al., 1980). Stock concentrations of ssDNA and dsDNA were determined by absorbance at 260 nm, with 36 and 50 $\mu g\ mL^{-1}\ A_{260}^{-1}$ as conversion factors, respectively. DNA concentrations are expressed as total nucleotides or as total molecules as noted. The plasmid pBR322 (Bolivar et al., 1977) was used as a heterologous substrate. The plasmid pMMC5 is the plasmid pXF3 (Maniatas et al., 1982) with a 307-bp *Bam*HI–*Cla*I fragment from wild-type bacteriophage M13 replacing the *Bam*HI–*Cla*I fragment of pXF3. Restriction enzymes were purchased from New England Biolabs. All other biochemicals and enzymes were purchased from Sigma.

Full-length linear dsDNA and duplex fragments were produced by cleaving plasmid or bacteriophage DNA with appropriate restriction enzymes. Isolation of individual duplex DNA fragments from an agarose gel was carried out as described (Dretzen et al., 1981). Nicked circular duplex DNA was prepared from bacteriophage DNA by the method of Shibata et al. (1981). All duplex DNA substrates employed in this study are shown in Figure 1.

Instrumentation. Absorbance measurements were obtained on a Perkin-Elmer Lambda 7 double-beam recording spectrophotometer equipped with two six-position thermojacketed cuvette holders attached to a constant-temperature water

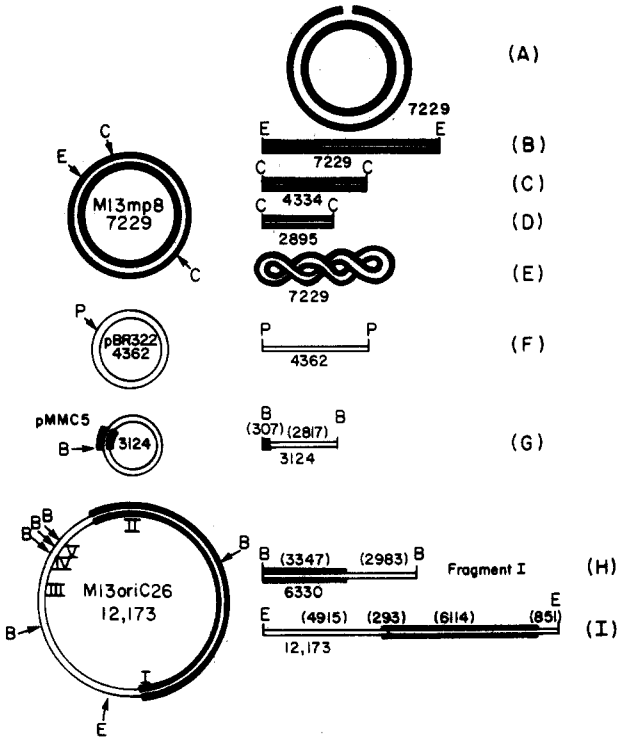


FIGURE 1: DNA substrates. Maps of duplex DNA molecules derived from bacteriophages M13mp8 and M13oriC26 and the plasmids pBR322 and pMMC5. Restriction enzyme digests and isolation and purification of DNA fragments are described under Materials and Methods. Letters in parentheses are used in the text to identify the substrate by which they appear. Letters without parentheses, B, C, E, and P, denote the restriction enzyme sites, *Bam*HI, *Cla*I, *Eco*RI, and *Pst*I, respectively. Roman numerals inside the circular M13oriC26 dsDNA represent each of the fragments obtained from a digest of this DNA with *Bam*HI. The total length in base pairs of each duplex substrate is indicated (numbers without parentheses). Thick lines represent regions of M13mp8 homology, and thin lines represent regions of heterology relative to M13mp8. Numbers in parentheses represent the length in base pairs of separate regions of heterology or homology relative to M13mp8 within each substrate as indicated. Linear molecules are oriented such that the 5′ end of the (+) strand is at the left.

circulator. Cell path length was equal to 1 cm when DNA and protein stock concentrations were determined and 0.5 cm during ATPase assays. The band-pass was equal to 2 nm at all times.

Reaction Conditions. All reactions were carried out at 37 °C in standard reaction buffer consisting of 25 mM Tris-HCl (80% cation, pH 7.5), 10 mM $MgCl_2$, 1 mM DTT, and 5% glycerol. Reaction mixtures, unless otherwise stated, contained 2 μM *recA* protein, 0.8 μM SSB protein, 8 μM ssDNA, 1 mM ATP, an ATP regenerating system (4.5 units/mL pyruvate kinase, 2.31 mM phosphoenolpyruvate, 0.44 mM KCl), and the indicated amounts of dsDNA.

ATPase Assays. Hydrolysis of ATP by *recA* protein was measured by a coupled spectrophotometric assay, which is described elsewhere (Morrical et al., 1986). This assay represents a significant improvement in accuracy and reproducibility relative to methods based on labeled ATP. Lactate dehydrogenase (4.5 units/mL) and 1.0 mM NADH were added to the standard ATP regenerating system to form the coupling system. The conversion of NADH to NAD was then followed spectrophotometrically. NADH absorbance was monitored at 370 nm instead of 340 nm, its absorbance maximum, in order to accommodate the high concentration of NADH needed to reach steady state while remaining in the linear range of the spectrophotometer. Reactions were carried out in cuvettes with a 0.5-cm path length for the same reason. Absorbance values at 370 nm were highly reproducible despite the steepness of the NADH absorbance spectrum in this region. Rates of ATP hydrolysis, expressed as micromolar ATP hydrolyzed per minute, were calculated from $-\Delta A_{370}$ per minute data by using an extinction coefficient of $\epsilon_{370} = 2.64$ mM^{-1} cm^{-1} for NADH. Error from all sources in steady-state rates of ATP hydrolysis was generally less than 5% in experiments carried out on different days. Reaction volumes of 0.4 or 0.5 mL were contained in 0.5-mL cuvettes. Unless otherwise noted, *recA* protein, coupling system, and DNA substrates were preincubated in reaction buffer for 10 min at 37 °C, and ATP hydrolysis was then initiated by the addition of a mixture of ATP and SSB protein. In many cases (as noted) duplex DNA was added after the addition of ATP and SSB. The total change in reaction volume resulting from this addition was less than 1%; therefore, no correction was made for dilution. Since ATP is regenerated constantly in the assay, conversion of NADH to NAD reflects the initial rate of ATP hydrolysis at all times. Increasing the concentration of ATP or any of the coupling system components in no case affected the observed rate of ATP hydrolysis in this assay, so that data reflect the maximum velocity of ATP hydrolysis at ATP saturation under all conditions used in this study. A short lag (less than 2 min) due to the coupling system is always observed in this assay before steady-state conversion of NADH to NAD is obtained. The length of the coupling lag was evaluated in experiments employing ssDNA as a cofactor for *recA* protein promoted ATP hydrolysis. This ssDNA-dependent ATP hydrolysis exhibits no significant lag when measured by other assays. In experiments in which a lag in ATP hydrolysis is observed and measured with both single-stranded and double-stranded DNA, the system lag measured in the presence of ssDNA was substracted from all data.

Agarose Gel Assay for DNA Strand Exchange. The formation of the nicked circular heteroduplex (FII) product of strand exchange was monitored by the agarose gel electrophoresis assay of Cox and Lehman (1981a). Aliquots (10 μL) of the reaction mixture, taken at the indicated times, were added to a gel loading buffer containing 12 mM EDTA, 1% SDS, 0.05% bromophenol blue, and 5% glycerol. The quenched reaction samples were immediately set on ice until all had been collected. Samples were loaded on a 0.8% agarose gel and electrophoresed in buffer containing 0.04 M Tris–acetate (pH 7.5) and 1 mM EDTA.

RESULTS

Hydrolysis of ATP Decreases When Strand Exchange Is Initiated. Strand exchange is initiated by the homologous pairing of the duplex DNA with the presynaptic *recA*–ssDNA complex. To compare ATP hydrolysis before and during strand exchange, *recA*–ssDNA complexes were formed initially in the absence of duplex DNA. This permitted the establishment of a base-line rate of ATP hydrolysis by the *recA*–ssDNA complex prior to initiation of strand exchange. This initial period also included the short lag in ATP hydrolysis attributable to the coupling system. Therefore, this system lag has no effect on the results described below.

The effects of the addition of linear dsDNA on the hydrolysis of ATP by the *recA*–ssDNA complex are presented in Figure 2. The arrow in each panel indicates the time at which the duplex DNA is introduced. Experiments in panels A and B represent experiments carried out at two different concentrations of complexes, although the stoichiometries of the components are the same in both cases. In panel A, curve a is the control representing ATP hydrolysis by *recA* nucleoprotein filaments on M13mp8(+) ssDNA. To duplicate the

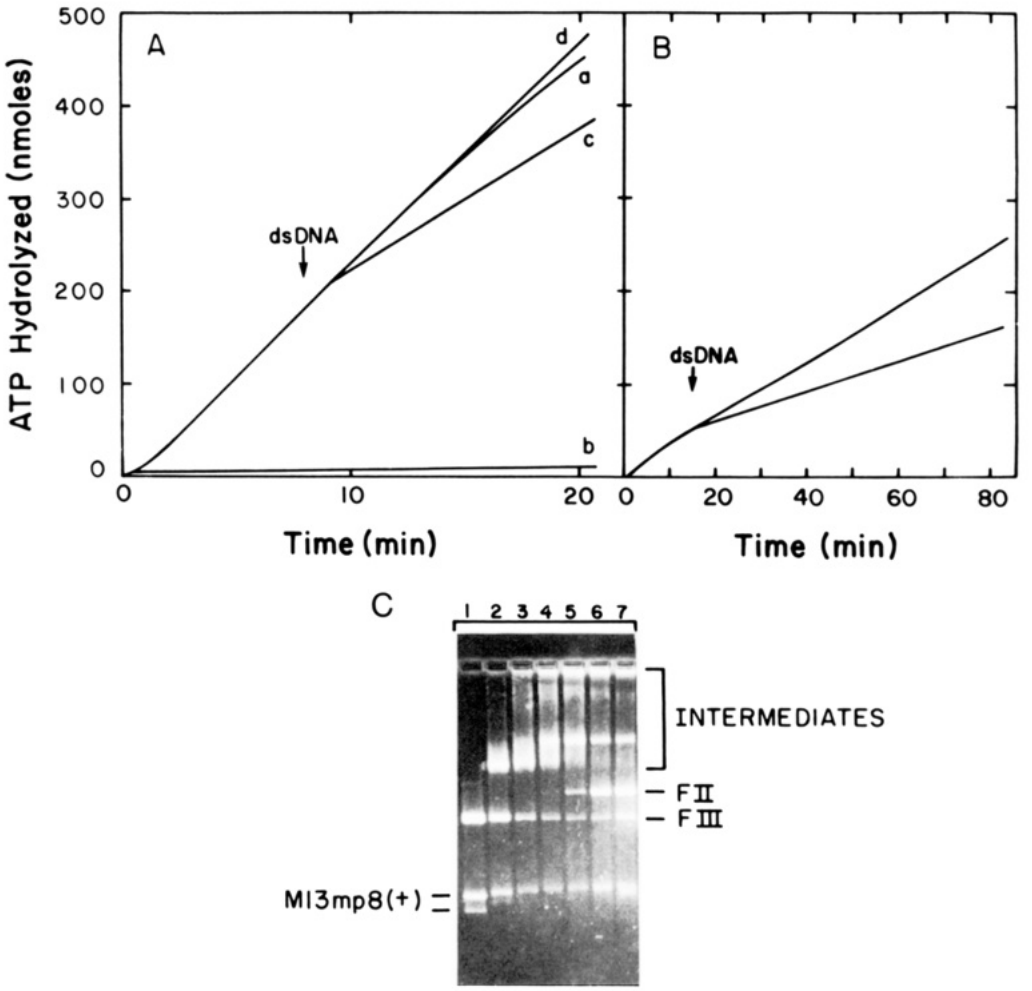


FIGURE 2: Effect of duplex DNA on ATP hydrolysis by the *recA*–ssDNA complex. ATPase reactions were performed as described under Materials and Methods except that duplex DNA or an equivalent volume of TE was added to preformed *recA*–ssDNA complexes. Reactions in panel A contained the standard reaction mixture (0.5 mL) without duplex DNA. At the arrow, the following additions were made in 4-μL volume: (a) TE; (b) ssDNA absent, linear M13mp8 dsDNA; (c) linear M13mp8 dsDNA; (d) linear pBR322 dsDNA. The final concentration of duplex DNA resulting from the addition was 16 μM in total nucleotides. In panel B, reaction mixtures (0.5 mL) contained 0.5 μM *recA* protein, 0.2 μM SSB protein, 2 μM M13mp8(+) ssDNA, and all other components as above. Linear M13mp8 dsDNA (bottom curve) or linear pBR322 dsDNA (top curve) was added in 4 μL to a final concentration of 4 μM in total nucleotides. Panel C contains a gel assay of a strand exchange reaction carried out under the conditions as in reaction c of panel A. Lane 1 is ssDNA and linear dsDNA markers at a concentration equivalent to that used in the reaction. Lanes 2–7 are time points taken at 5, 10, 15, 20, 30, and 60 min, respectively. FIII and FII represent the linear dsDNA substrate and the nicked circular dsDNA product for the reaction. The ssDNA marker was not incubated at 37 °C and migrates as a doublet in this gel system, although greater than 95% of the ssDNA is circular (not shown). The bottom band is lost when the ssDNA is exposed to 37 °C briefly and cooled quickly as in this assay (lanes 2–7), suggesting it is a species that migrates faster because of differences in secondary structure.

slight volume changes produced by the duplex DNA additions in the other experiments, 4 μL of TE buffer [10 mM Tris (80% cation, pH 7.5), 1 mM EDTA] was added to this mixture at the time indicated by the arrow. The rate of ATP hydrolysis remains essentially unchanged, although a slight decline is observed at later times in the reaction. This slight decline does not occur in the presence of heterologous duplex DNA (see below), and the basis for it is unclear. In curve b, ssDNA is omitted, and linear M13mp8 dsDNA (Figure 1B) is added at the time indicated by the arrow to evaluate the dsDNA-dependent ATPase levels under these conditions. Over this time course very little ATP hydrolysis is observed. Similar results have been previously reported by Pugh and Cox (1987a). Under these conditions direct binding of *recA* protein to duplex DNA is slow enough to be nearly negligible on this time scale. If this same amount of linear M13mp8 dsDNA is added to the complexes of *recA* protein, SSB protein, and M13mp8(+) ssDNA, the resulting rate of ATP hydrolysis was not found to be the sum of the ssDNA- and dsDNA-dependent ATP hydrolyses observed in experiments a and b. Instead, the rate of ATP hydrolysis decreases by 33%. This decrease is complete in less than 2 min (curve c). After this drop, the rate of ATP hydrolysis again becomes constant. The short time span required to complete this drop correlates well with the time required to complete the synapsis phase of DNA strand exchange (Cox et al., 1983a; Kahn & Radding, 1984; Riddles & Lehman, 1985). An agarose gel assay carried out under the same conditions (panel C, lanes 1–7) confirmed that this reaction results in efficient strand exchange. A band corresponding to the nicked circular heteroduplex product (FII) is observed at 20 min. As shown in curve d, the drop in ATP hydrolysis described above is completely homology dependent. In this reaction heterologous linear pBR322 dsDNA (Figure 1, F) is substituted for the linear M13mp8 dsDNA, and no decline in ATP hydrolysis is observed. In fact, the addition of heterologous DNA appears to have a slight stabilizing effect on the rate of ATP hydrolysis by these complexes (compare a and d). No reaction with this heterologous substrate was observed by the agarose gel assay for strand exchange (not shown). The homology dependence and

the time course of the drop in ATP hydrolysis suggest that this effect is associated with some event in the synapsis phase of strand exchange. At a minimum, the decrease in ATP hydrolysis is kinetically competent to reflect an important event in this phase.

The limitations imposed by the spectrophotometer do not permit observation of ATP hydrolysis via the coupled assay for more than 20 min under these conditions. By lowering the concentration of *recA* protein, SSB protein, ssDNA, and dsDNA (relative stoichiometries are maintained), the length of the time course was extended. The extended time course is shown in panel B of Figure 2. After addition of homologous linear dsDNA, indicated by the arrow, the rate of ATP hydrolysis again decreases 33% within 2 min, and the new (lower) rate of ATP hydrolysis was then maintained for at least 60 min (lower curve). As before, strand exchange is nearly complete within 30 min (not shown). Therefore, no additional change in the rate of ATP hydrolysis is observed during strand exchange. Continuation of this rate well beyond the completion of strand exchange indicates continued binding of *recA* protein to DNA. This complements the data of Pugh and Cox (1987b), which demonstrated by several other methods that *recA* protein remains bound to the heteroduplex product of strand exchange. As a control, heterologous linear dsDNA was again added at the indicated time (upper curve), and no change in ATPase activity was observed. We carried out the same set of experiments in a reaction buffer with the same ionic strength but with acetate anions replacing chloride anions. A comparable drop in ATP hydrolysis was again observed when homologous dsDNA was introduced (data not shown), demonstrating that this effect is not limited to one set of ionic conditions.

Decrease in ATP Hydrolysis Reflects Interaction of One Molecule of Duplex DNA with Each recA–ssDNA Complex. This homology-dependent effect could involve one or multiple molecules of duplex DNA. It seemed possible, in fact, that the effect observed in Figure 2 is not the maximum possible effect. The addition of more homologous duplex DNA might decrease the rate of ATP hydrolysis further, perhaps leading to a large increase in the apparent efficiency of DNA strand exchange. A fixed concentration of *recA*–ssDNA complexes was therefore titrated with homologous duplex DNA. For all titration experiments in this report, both the ssDNA and the duplex DNA were added to the preincubation mixture. Strand exchange was then initiated by the introduction of a mixture of ATP and SSB.[2] Rates of ATP hydrolysis were recorded after steady state had been achieved (after t = 4 min), and the results are presented in Figure 3. Each point on the curve represents an individual ATPase assay except the point representing zero dsDNA (open triangle), which is an average value of 18 assays carried out on 16 days. The vertical height of this symbol corresponds to the standard deviation of this experiment. As shown in Figure 3, saturation behavior is clearly observed. With full-length linear M13mp8 dsDNA (Figure 1, B), the 33% drop is the maximum decline observed, and this saturation point is reached when 1 ± 0.1 duplex DNA molecule is present for each *recA*–ssDNA complex present (Figure 3, open circles). The calculated apparent stoichiometry is equal to the molar ratio of dsDNA and ssDNA molecules obtained at the intersection of a line drawn through the "plateau" region of the titration curve and the best line drawn through the linear descending portion of the titration curve.

[2] Rates of ATP hydrolysis obtained with this protocol were identical with those obtained when duplex DNA was the last component added.

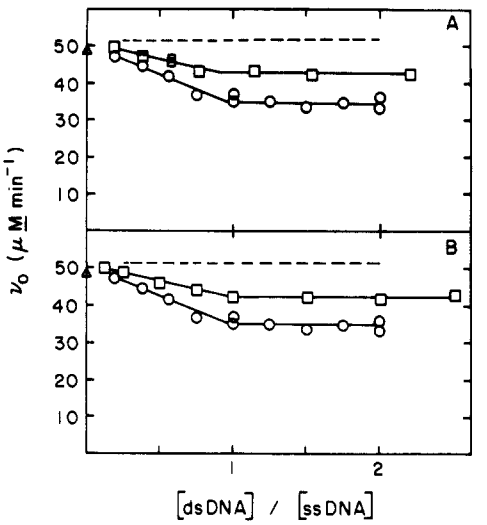


FIGURE 3: Duplex DNA-dependent drop in ATP hydrolysis by *recA*–ssDNA complexes: effect of homologous linear dsDNA concentration. Titration curves were obtained as described in the text. Reactions were run under standard conditions in 0.4 mL with duplex DNA added to the preincubation mixture as described under Materials and Methods. Each point represents a separate experiment, except the point at zero duplex DNA (open triangle, panels A and B), which is an average of 18 assays. Duplex DNA concentrations are expressed as the ratio of total duplex DNA molecules to total ssDNA molecules in the final reaction mixture. The duplex DNA substrates employed are full-length M13mp8 (open circles, panels A and B), small *Cla*I fragment of M13mp8 (open squares, panel A), and large *Cla*I fragment of M13mp8 (open squares, panel B). The dashed line represents a titration with heterologous linear pBR322 dsDNA (data are reported in Figure 6). The estimated equivalence point for each titration is indicated by the intersection of asymptotic lines drawn on the plot. The parameter v_0' represents the limiting value of v_0 at saturation with respect to a given duplex DNA substrate.

These data indicate that all of the *recA*–ssDNA complexes are involved in the homologous pairing that results in this drop in ATP hydrolysis. The overall strand exchange reaction results in conversion of 60–70% of these substrates into products when sufficient duplex DNA is present (see, e.g., Figure 2C).

M13mp8 dsDNA can be further subdivided into two *Cla*I fragments, representing 60% and 40% of the parent molecule (Figure 1, C and D, respectively). Additional titrations were carried out with these fragments after separation and purification as described under Materials and Methods. The open squares in panel A represent a titration curve with the small *Cla*I fragment of M13mp8. A similar titration with the large *Cla*I fragment of M13mp8 is shown in panel B (open squares). In both cases a decline in ATP hydrolysis is again observed, which shows saturation when 1 ± 0.1 duplex fragment is present for each *recA*–ssDNA complex. The total decrease observed with these fragments, however, is significantly less than that observed with the full-length duplex. This is explored further in the next section. The invariant nature of the observed 1:1 stoichiometry at saturation provides confirmation that the drop in ATP hydrolysis involves all of the *recA*–ssDNA complexes in the reaction mixture rather than a subset of them. As a control, a titration with linear pBR322 dsDNA was performed (dashed line, panels A and B). No decrease in ATP hydrolysis was observed with this heterologous substrate, confirming that this effect is completely homology dependent. In every separate experiment described in this study the final rate of ATP hydrolysis was achieved in less than 2 min after the initiation of strand exchange.

Extent of Decrease in ATP Hydrolysis Is Directly Related to the Length of Homology. In the experiments described in

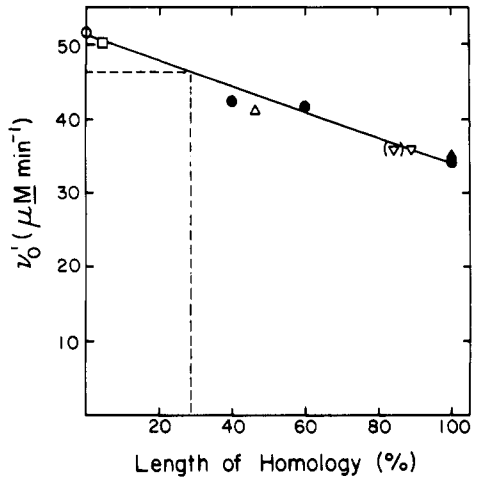


FIGURE 4: Relationship between the duplex DNA dependent decrease in ATP hydrolysis and the length of homology. Values for v_0' were obtained as described in the text and in the legend of Figure 3. Values for completely homologous linear dsDNA (closed circles) correspond to full-length M13mp8 (100%), the large *Cla*I fragment of M13mp8 (60%), and the small *Cla*I fragment (40%). These are substrates B, C, and D, respectively, in Figure 1. Other points correspond to heterologous linear pBR322 dsDNA (open circle), chimeric linear dsDNA, pMMC5 (open square), fragment I of M13oriC26 (open triangle), and *Eco*RI linearized M13oriC26 (open inverted triangle with and without parentheses, see text for details). These are substrates F, G, H, and I, respectively, in Figure 1. The closed triangle corresponds to an equimolar mixture of both the large and small *Cla*I fragments (see text for details). The dashed line represents a determination of the length of homology available for pairing for supercoiled M13mp8 dsDNA as described in the text. This is substrate E in Figure 1.

Figure 3, an apparent correlation is evident between the length of the homologous dsDNA molecule and the extent of the decrease in the rate of ATP hydrolysis. This suggests that the decline in ATP hydrolysis is related not only to the homologous interaction but to the length of available homology. To explore this possibility further, it is necessary to define a new kinetic parameter, v_0'. This is the steady-state rate of ATP hydrolysis at saturation with respect to duplex DNA molecules and is equal to the rate of ATP hydrolysis at the "plateau" region of the titration curves in Figure 3. A higher value for v_0' (smaller decrease) is observed for the *Cla*I fragments than for the full-length linear M13mp8 duplex. This trend is continued by the completely heterologous linear pBR322 dsDNA, which shows no decrease in ATPase activity. When the values of v_0' from each of the titration curves in Figure 3 are plotted vs. the percent length of homology relative to M13mp8(+) ssDNA, a linear relationship is revealed (closed circles, Figure 4).

Since DNA molecules with both homologous and heterologous sequences have not yet been included, it is not clear whether this relationship reflects the total length of available homology. It is possible that only a short region of homology is required, and the relationship of Figure 4 would then reflect the total length of any DNA molecule containing some homology. To distinguish between these possibilities, chimeric duplex DNA substrates were employed in these experiments. If the duplex DNA derived from the bacteriophage M13oriC26 is cleaved with *Bam*HI, it is possible to isolate a fragment that is only partially homologous to M13mp8(+) ssDNA. This chimeric substrate contains 3347 base pairs of homology at the 5′ end with respect to the (+) strand and a 2983 base pair heterologous tail (Figure 1, H). This substrate was titrated into a series of reaction mixtures as described above to determine if the drop in ATP hydrolysis would correspond to the entire length of the duplex or to the homologous portion alone. The results of this experiment are shown in Figure 5 (closed squares). The value of v_0' from this titration curve was equal to 41.2 μM min^{-1}, which represents only a partial decrease with respect to the value of v_0' for full-length linear M13mp8 dsDNA, 34.2 μM min^{-1} (dashed line). Since the length of this chimeric substrate (6330 bp) is only slightly less than that of M13mp8 dsDNA (7229 bp), this drop must not reflect the entire length of the chimeric dsDNA. However, this v_0' value does correspond well with the homologous portion of the molecule (open triangle, Figure 4). The effect of this substrate also exhibits saturation at an apparent stoichiometry of 1 ± 0.1 dsDNA molecule for each *recA*–ssDNA complex. We carried out the same analysis with another chimeric plasmid, pMMC5. When linearized with *Bam*HI, this substrate has an homologous region of 307 base pairs at its 5′ end with respect to the (+) strand and a 2817 base pair heterologous tail (Figure 1, G). The v_0' value obtained from its titration curve (not shown) is equal to 50.3 μM min^{-1}, a negligible decrease that again corresponds well with the short length of available homology in this substrate (open square, Figure 4). The very small decrease obtained with pMMC5 dsDNA did not permit a determination of the dsDNA–complex saturation point for this substrate. These results demonstrate that the decrease in the rate of ATP hydrolysis is completely dependent upon the *length* of available homology in the duplex DNA. These results are not an artifact restricted to M13mp8 DNA. Similar results have been obtained with *recA* complexes formed on ssDNA derived from bacteriophages ϕX174 and M13oriC26 (Brenner et al., 1987; B. C. Schutte, unpublished results).

This correlation is strengthened further by the observation that the effects of the two *Cla*I fragments of M13mp8 dsDNA as described above are additive. When both fragments were added to the *recA*–ssDNA complexes in equal molar amounts, the decrease in ATP hydrolysis was equivalent to that observed with full-length linear M13mp8 dsDNA (closed triangle, Figure 4). This demonstrates that homologous sequences in the duplex do not have to be covalently contiguous to bring about this effect. It also demonstrates that *recA* monomers in different parts of the *recA*–ssDNA complex can act independently. The results suggest that strand exchange can occur at more than one point simultaneously in a single complex. This is supported by the observation that the rate of formation of heteroduplex DNA is doubled when both *Cla*I fragments of M13mp8 are present in a standard reaction mixture (B. C. Schutte, unpublished results).

The slope of the line in Figure 4 corresponds to a 33% decrease in the rate of ATP hydrolysis involving *recA* monomers throughout the length of M13mp8 homology contained in the duplex substrate. This relationship, along with the fact that the effect is always complete in less than 2 min and exhibits saturation with one duplex DNA fragment or molecule per *recA*–ssDNA complex, leads directly to the conclusion that some form of homologous contact occurs between the *recA*–ssDNA complex and the entire homologous length of the duplex DNA during the synapsis phase of strand exchange. The form of this homologous contact is explored in the next section.

Formation of a Paranemic Joint Is Sufficient To Produce a Decrease in Rate of ATP Hydrolysis. Up to this point all duplex DNA substrates used in these experiments could form homologous contacts through either a paranemic (nonintertwined) or a plectonemic (intertwined) joint. If the duplex substrate lacks a free end in the region of homology, then formation of a plectonemic joint is topologically forbidden.

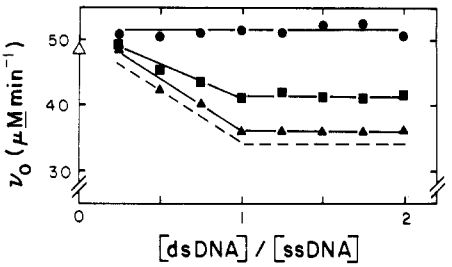


FIGURE 5: Duplex DNA dependent decrease in ATP hydrolysis by *recA*–ssDNA complexes: effect of heterologous and chimeric dsDNA concentration. Titration curves were obtained as described in the text and in the legend of Figure 3. The duplex DNA substrates employed are heterologous linear pBR322 dsDNA (closed circles), chimeric linear dsDNA, fragment 1 of M13oriC26 (closed squares), and *Eco*RI linearized M13oriC26 (closed triangles). These are substrates F, H, and I, respectively, in Figure 1. The open triangle represents a control in the absence of duplex DNA as described in Figure 3. The dashed line represents a titration with full-length M13mp8 dsDNA (data are reported in Figure 3). The hatch marks indicate the deletion of a portion of the vertical axis.

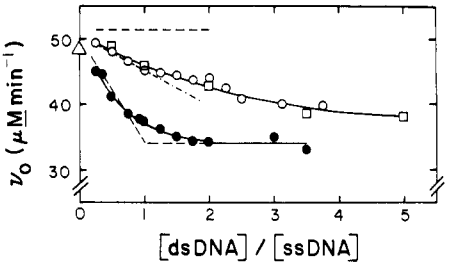


FIGURE 6: Duplex DNA dependent decrease in ATP hydrolysis by *recA*–ssDNA complexes: effect of homologous supercoiled and nicked circular dsDNA concentration. Titation curves were obtained as described in the text and in the legend of Figure 3. The duplex DNA substrates employed are supercoiled M13mp8 dsDNA (open symbols) and nicked circular M13mp8 dsDNA (closed circles). Two different supercoiled M13mp8 dsDNA preparations, differing in their content of nicked molecules, were employed: 15% nicked molecules (open circles) and 5% nicked molecules (open squares). Curves are drawn through all data points (solid line) and through the initial slope (dash–dot line). See text for details. The open triangle has the same representation as in Figure 3. The dashed lines are titrations with full-length homologous M13mp8 dsDNA (lower curve) and heterologous pBR322 dsDNA (upper curve) (data are reported in Figures 3 and 5, respectively). The hatch marks indicate the deletion of a portion of the vertical axis.

However, pairing via a paranemic joint can still occur (Das-Gupta et al., 1980; Christiansen & Griffith, 1986). We tested two such duplex DNA substrates: the chimeric M13oriC26 dsDNA, linearized by *Eco*RI such that the 6407-bp homologous region was flanked at each end with a long heterologous region (Figure 1, I), and supercoiled M13mp8 dsDNA (see next section). The titration of a constant amount of *recA*–ssDNA complexes by *Eco*RI-linearized M13oriC26 dsDNA is shown in Figure 5 (closed triangles). As in every other case, the drop in ATP hydrolysis with this substrate exhibits saturation with an apparent stoichiometry of 1 ± 0.1 duplex DNA molecule for each complex. Moreover, the extent of the drop indicates that the relationship between v_0' and the length of homology described above exists even for this substrate (Figure 4, open inverted triangle). Therefore, formation of a paranemic joint is sufficient to cause the full decrease in the rate of ATP hydrolysis. It should be noted that M13oriC26 is a derivative of wild-type M13 bacteriophage and so does not contain in its genome the approximately 820 base pair region corresponding to the polylinker region and the *lac* Z gene sequences in bacteriophage M13mp8. This means the homology between M13mp8(+) ssDNA and this duplex substrate consists of 293 and 6114 base pair regions effectively separated by an 820 base pair insertion in the ssDNA. The site corresponding to this insertion is denoted in the M13oriC26 dsDNA by a vertical line near the 5′ end [with respect to the (+) strand] of the homologous region in Figure 1, I. Whether both sides of homology are paired simultaneously cannot be determined by these experiments as the difference in the length of total homology, 6407 base pairs, and continuous homology, 6114 base pairs, is too small for detection in these experiments. Points corresponding both to the total homology (open inverted triangle) and the somewhat shorter continuous homology (in parentheses) are plotted in Figure 4.

Incoming dsDNA Molecule in the Paranemic Complex Is Unwound. We also tested supercoiled M13mp8 dsDNA (Figure 1, E), which, because it also lacks a free end, forms only a paranemic joint with M13mp8(3) ssDNA. However, this substrate has the added constraint of being covalently closed. Thus, the unwinding of the duplex DNA that may accompany the formation of a paranemic joint [e.g., Wu et al. (1983)] is limited by topological strain. We asked whether this added restriction on the length of a potential paranemic joint would result in a less dramatic decrease in ATP hydrolysis. Figure 6 shows the results of a titration of a constant concentration of *recA* protein and M13mp8(+) ssDNA complexes by supercoiled M13mp8 dsDNA. Comparison of results obtained with heterologous (top dashed curve) and homologous (bottom dashed curve) linear dsDNA shows that the decrease in ATP hydrolysis due to paranemic pairing by the supercoiled dsDNA does occur, but at a reduced level. At a stoichiometry equal to 1, the rate of ATP hydrolysis has decreased to 46 μM min^{-1}. If the curve in Figure 4 is used as a standard, this value of v_0' corresponds to 27.5% (dashed line) of the decrease observed with full-length M13mp8 dsDNA. A decrease of this magnitude would correspond to a paranemic joint about 2000 base pairs in length. This result was repeated with two different preparations of supercoiled M13mp8 DNA with similar results. Since these contained different amounts of nicked circular duplex molecules (15% and 5%, open squares and open circles, respectively), we believe this result was affected minimally by the small amount of relaxed duplex DNA present.

The effect observed with supercoiled dsDNA was unique in another respect. While linear M13mp8 dsDNA exhibits saturation at a stoichiometry of 1:1, the titration curve of supercoiled dsDNA continues to decrease beyond a stoichiometry of 1:1, suggesting that more than one of these circular duplex molecules can pair with each nucleoprotein filament. This might be expected if only 2000 of the 7229 base pairs of M13mp8(+) ssDNA in the complex are paired by any one supercoiled duplex molecule. Thus, the extent of the drop in ATP hydrolysis approaches v_0' for the linear M13mp8 dsDNA at high concentrations of the supercoiled duplex substrate. However, formation of paranemic joints with additional molecules of supercoiled M13mp8 dsDNA appears to become less efficient as the concentration of duplex DNA increases above a molar ratio of 1. The 2000 base pair length for these paranemic joints is based on the initial slope of the titration curve in Figure 6 (dash–dot line). The gradual change in this slope may indicate an inhibitory steric interaction between supercoiled dsDNA molecules paired with the same complex.

The partial decrease in the rate of ATP hydrolysis brought about by the homologous supercoiled dsDNA is consistent with the hypothesis that the incoming dsDNA molecule is underwound in a paranemic joint. If the topological restraint to unwinding is removed, this hypothesis would predict a longer paranemic joint and a greater drop in the rate of ATP hydrolysis. To test this, supercoiled M13mp8 dsDNA was nicked

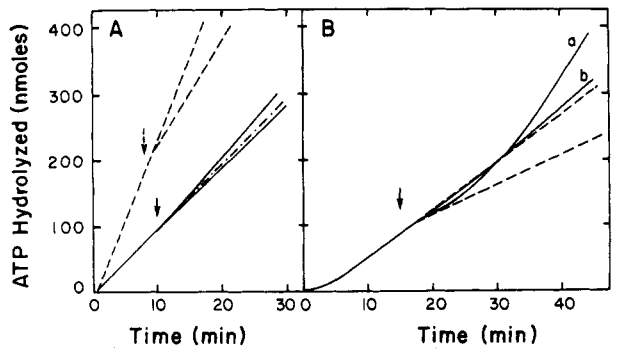


FIGURE 7: Effect of duplex DNA on ATP hydrolysis: effect of SSB and *recA* protein concentration. ATPase reactions were performed as described under Materials and Methods and in the legend of Figure 2. Reactions in panel A contained the standard reaction mixture without SSB and duplex DNA. At the arrow the following additions were made in 4-μL volume: TE (dash–dot curve); linear M13mp8 dsDNA (top curve); linear pBR322 dsDNA (bottom curve). The final concentration of duplex DNA resulting from the addition was 16 μM in total nucleotides. For comparison, the dashed curves represent ATP hydrolysis in the presence of SSB and in the absence (top) or presence (bottom) of homologous dsDNA (data are reproduced from Figure 2A). In panel B, reaction mixtures contained the standard concentrations of all components except ssDNA, which was 2 μM. Linear M13mp8 dsDNA (curve a) or linear pBR322 dsDNA (curve b) was added in 4 μL to a final concentration of 16 μM in total nucleotides. The dashed curves represent ssDNA-dependent ATP hydrolysis (top dashed curve) and the predicted ATP hydrolysis after a homology-dependent drop analogous to that observed in Figure 2A (bottom dashed curve).

as described under Materials and Methods. The titration of a constant amount of *recA*–ssDNA complexes with nicked circular M13mp8 dsDNA (Figure 1, A) is shown in Figure 6. To a first approximation, this titration curve (closed circles) resembles the linear dsDNA titration curve (bottom dashed curve), exhibiting an apparent stoichiometry of 1 ± 0.1 duplex DNA molecule for each complex and a value of ν_0' equal to 34.5 μM min^{-1}. Thus, unlike the supercoiled substrate, all homologous sequences in the nicked circular dsDNA appear to be available for paranemic pairing. This suggests that the only major topological restraint to the formation of a paranemic joint with a supercoiled dsDNA is unwinding of the duplex. We note that the equivalence point for the nicked circular dsDNA titration curve is not as sharp as observed with the linear dsDNA. This may suggest that a weaker complex is formed with the nicked molecules than is observed with linear duplexes.

Effects of SSB and recA Protein Concentration. The results described above can be significantly altered by any free *recA* protein present in the reaction mixture. This can occur either by omitting SSB or by using an excess of *recA* in the presence of SSB. SSB protein is required for optimal strand exchange and for the stable maintenance of *recA*–ssDNA complexes (Morrical & Cox, 1987). We have nonetheless attempted to observe these homology-dependent effects on ATP hydrolysis in its absence (Figure 7A). As shown previously (Morrical et al., 1986), the rate of ssDNA-dependent ATP hydrolysis in the absence of SSB (dash–dot curve) is markedly less than that in its presence (top dashed curve). This is due to the exclusion of *recA* protein from regions of secondary structure when SSB is omitted (Muniyappa et al., 1984), with the result that some of the *recA* protein present under standard conditions is not bound to DNA. Introduction of linear M13mp8 dsDNA at the indicated time under these conditions causes a slight increase in the rate of ATP hydrolysis (top curve), instead of the decrease observed in the presence of SSB (bottom dashed curve). This small stimulation of ATP hydrolysis is not observed in the heterologous control (bottom curve). These effects appear to reflect binding of the excluded *recA* protein to DNA. When protocols were employed [a Mg shift; see Muniyappa et al. (1984)] that permit more complete binding of *recA* protein to the ssDNA without SSB, the homology-dependent decrease in ATP hydrolysis in response to added duplex was again observed (not shown). However, regardless of the protocol used, *recA* complexes on ssDNA are unstable when SSB is omitted (Morrical & Cox, 1987), and the results obtained were found to be subject to greater error.

We also carried out the same set of experiments with excess *recA* protein added in the presence of SSB (Figure 7B). *recA* protein binds ssDNA at a stoichiometry of one monomer per four nucleotides (Cox & Lehman, 1987). The standard reaction mixture used up to this point contains 2 μM *recA* protein and 8 μM M13mp8(+) ssDNA. For this set of experiments, the concentration of M13mp8(+) ssDNA was reduced to 2 μM, thus yielding a fourfold excess of *recA* protein. Addition of linear M13mp8 dsDNA (curve a) to this reaction mixture causes a drop in the rate of ATP hydrolysis similar to that observed for reactions containing stoichiometric amount of *recA* proteins (bottom dashed curve). However, this lower rate is not maintained. Rather, it begins to increase, and after 10 min a new steady-state rate of ATP hydrolysis is achieved that is greater than the rate in the presence of ssDNA alone (top dashed curve). This secondary effect is largely homology dependent. ATP hydrolysis increases slightly when linear pBR322 dsDNA is introduced (curve b). This additional ATP hydrolysis is not important to the strand exchange reaction, as efficient strand exchange occurs without excess *recA* protein (Figure 2C). Again, this effect reflects the excess *recA* protein present in this reaction mixture. This effect will be described in detail elsewhere. Our purpose here is simply to point out that the effects described in this paper can be masked by secondary reactions unrelated to strand exchange if excess *recA* protein is present in the reaction mixture.

Discussion

The basic conclusion of this study is that early in strand exchange a paranemic joint is formed between the *recA*–ssDNA complex and the homologous duplex DNA. In this paranemic joint, homology is detected over the entire length of the available homology—over 7000 base pairs in the experiments reported here. This conclusion is based on the relatively simple observation that the initiation of strand exchange is accompanied by a reproducible decline in the rate of ATP hydrolysis by *recA* protein. Our extrapolation from this observation to the final conclusion is based on a careful examination of the properties of this change in ATP hydrolysis. The effect has five important properties that implicate it in the formation of paranemic joints during the synapsis phase of strand exchange and provide information about the structure of the paranemic complex. (1) It is completely homology dependent. No decrease in ATP hydrolysis is observed when heterologous linear dsDNA is added. This inseparably ties this effect to the most basic of *recA* protein activities—the pairing of DNA strands. (2) This effect occurs in less than 2 min, which correlates well with the time required for synapsis. The effect is therefore kinetically competent to reflect an event associated with the formation of paranemic joints. After this initial drop, no further change in ATP hydrolysis occurs, and the rate remains constant well after strand exchange is complete. (3) The effect exhibits saturation at a stoichiometry of 1 ± 0.1 linear dsDNA molecule for every *recA* nucleoprotein filament. This is true for full-length linear M13mp8 DNA, for shorter fragments of duplex M13mp8

DNA, and for a number of chimeric DNA substrates. (4) The rate of ATP hydrolysis at saturation with respect to the duplex DNA, v_0', is directly related to the *length of homology* in the duplex substrate. When chimeric DNA is employed, only the homologous portion affects ATP hydrolysis. This relationship implies synapsis occurs throughout the homologous region regardless of size. (5) This relationship is observed even when the pairing interaction is restricted to paranemic joints formed between the circular ssDNA and a linear dsDNA whose homologous region is flanked on both ends with extensive heterologous sequences. Therefore, the decrease in ATP hydrolysis that occurs when strand exchange is initiated reflects an event associated with the formation of paranemic joints.

These results apply to a range of DNA substrates and ionic conditions. We note two important factors, however, that cannot be varied. The presence of both SSB protein and a stoichiometric concentration of *recA* protein must be maintained. Whereas the changes we have noted are highly reproducible, they are small enough to be masked by secondary changes in the rate of ATP hydrolysis which can occur when these conditions are not met (see Results). This restriction does not detract from the basic conclusion described above. It simply results from the fact that *recA* protein promotes ATP hydrolysis in the absence of strand exchange. In order to observe changes in ATP hydrolysis related to strand exchange, it is necessary to eliminate, insofar as possible, any *recA* protein not directly involved in this reaction.

Paranemic Complexes Revealed by Homology-Dependent Changes in ATP Hydrolysis Are Longer Than Previously Estimated. Our results appear to conflict to varying degrees with previous estimates reported for the length of paranemic joints obtained with either linear or supercoiled dsDNA. By nuclease-sensitivity experiments, Bianchi et al. (1983) estimated a length of 500 bp for a paranemic joint, although the potential pairing length exceeded 7000 bp. In those experiments, however, SSB was absent. Since SSB has been shown to be required for maintenance of the *recA*–ssDNA complex (Morrical & Cox, 1987), the length of the paranemic joint may have been limited by a less stable *recA* nucleoprotein filament in that study. Christiansen and Griffith (1986) directly observed a 400-bp paranemic joint between a *recA*–ssDNA complex (formed in the presence of SSB) and a supercoiled dsDNA molecule by electron microscopy. This compares with 2000 bp detected in this paper with similar DNA substrates. The smaller estimate obtained from electron microscopy may reflect the loss of positive supercoils during fixation. Synapsis requires unwinding of the duplex (Wu et al., 1983; this paper). The unwinding required for a paranemic joint up to 400 bp could be accommodated by the unwinding already present in the supercoiled DNA. Unwinding in a longer paranemic joint would require the formation of compensatory positive supercoils which might have been disrupted during spreading. To a degree, these lower numbers may simply reflect the difficulty in obtaining accurate estimates when one is dealing with weak interactions, such as those in the demonstrably unstable paranemic joints. The real-time methods employed in this study are nondisruptive and optimize the stability of *recA*–ssDNA complexes.

Incoming Duplex in the Paranemic Complex Is Unwound. We note that pairing of the *recA*–ssDNA complex with the completely homologous supercoiled dsDNA led to only a partial drop in the rate of ATP hydrolysis, whereas the nicked circular dsDNA caused the full drop in ATP hydrolysis. This suggests that the only major topological restraint to the paranemic joint formed with the supercoiled substrate was unwinding. Rapid, homology-dependent unwinding of the incoming duplex has recently been observed directly (B. C. Schutte, unpublished results). A full-length paranemic joint with nicked circular dsDNA could not be formed if its structure resembled the intermediate proposed by Howard-Flanders et al. (1984) in which the *recA* filament wraps around all three DNA strands. Also inconsistent with a three-stranded helical structure are results from DNase protection experiments, which indicate that the duplex DNA substrate is completely sensitive to DNase at the point in the reaction in which formation of the paranemic complex is complete (Pugh & Cox, 1987b). Since the ssDNA is insensitive to DNase at the same point in time, these results indicate that the ssDNA is located inside the complex but the paired dsDNA is outside the complex. Among structures not previously proposed for the paranemic complex is one in which the DNA molecules are aligned side by side as shown in Figure 8. In this structure homologous contacts are periodic rather than continuous, occurring once per helical turn where bases are juxtaposed (arrows). A more detailed description of this structure is provided elsewhere along with a proposed mechanism for *recA* protein promoted strand exchange (Cox et al., 1987).

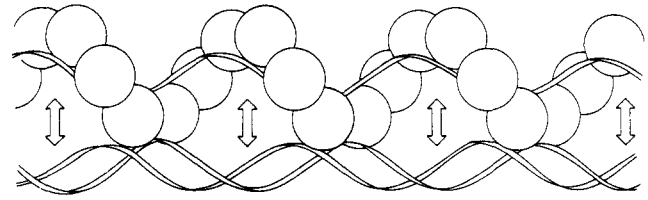


FIGURE 8: Proposed structure of the paranemic complex formed when *recA* protein promoted strand exchange is initiated. See Discussion for details.

Molecular Basis for This Homology-Dependent Change in Rate of ATP Hydrolysis Is Unknown. Morrical et al. (1986) have shown previously that SSB protein stimulates ATP hydrolysis by the *recA*–ssDNA complex. It was therefore conceivable that the effect we observed might be due to the loss of this stimulation by the displacement of SSB protein from the complex. However, using the intrinsic fluorescence of SSB protein as described previously (Morrical et al., 1986), we have demonstrated that the homology-dependent change in ATP hydrolysis does not reflect dissociationof SSB protein from the complex. Instead these experiments reveal a slow transfer of SSB to the displaced (+) strand concomitant with the progress of strand exchange (B. C. Schutte, unpublished results). The effect also does not reflect dissociation of a segment of the *recA* nucleoprotein filament at the site where strand exchange is being initiated. The length dependence of the effect clearly indicates that the change is occurring throughout the complex. And, the decrease in ATP hydrolysis produced by the entire linear M13mp8 duplex is the same whether it is introduced as a single molecule or as a mixture of several nonoverlapping fragments. Also, Christiansen and Griffith (1986) observed no changes in the ultrastructure of the *recA* filament induced at the site of formation of the paranemic joint. These are the only possibilities we have explored to date. We do not yet know if the extent of the drop, 33% over the length of the paranemic complex, has mechanistic significance. We note that the lower rate is similar to that observed when *recA* protein is bound entirely to duplex DNA (Pugh & Cox, 1987a). An obvious possibility is that paranemic joint formation is accompanied by a change in the state of the *recA* complex, which is then maintained throughout strand exchange.

Relationship to Other Aspects of recA Protein Promoted Strand Exchange. We note that the effect we have described

here involves an activity of *recA* protein, i.e., ATP hydrolysis. The DNA length dependence of this effect implies that *recA* monomers throughout the nucleoprotein filament are directly involved in the paranemic complex. This observation strongly supports the conclusion of Brenner et al. (1987) that ATP hydrolysis occurs throughout a nucleoprotein filament rather than being restricted to *recA* monomers at filament ends. The observation that this rate of ATP hydrolysis continues even after strand exchange is completed complements the observations of Pugh and Cox (1987b), which demonstrate that *recA* protein remains bound to the heteroduplex product.

Roman and Kowalczykowski (1986) have recently noted that a correlation can be drawn between rates of dsDNA-dependent ATP hydrolysis and DNA strand exchange as ionic conditions were varied. They suggested that ATP hydrolysis during strand exchange was composed of ssDNA and dsDNA components and that only the minor dsDNA-dependent component was relevant to the mechanism of DNA strand exchange. We show here that when homologous duplex DNA is added to a reaction mixture under conditions optimal for strand exchange, the rate of ATP hydrolysis *decreases* significantly. This indicates that there is no ssDNA-dependent component of ATP hydrolysis during strand exchange that can be separated from the total. Elsewhere, we describe a mechanism for *recA* protein promoted DNA strand exchange that provides a mechanistic role for all of the observed ATP hydrolysis in this reaction (Cox et al., 1987).

Registry No. ATP, 56-65-5; ATPase, 9000-83-3.

REFERENCES

Bianchi, M., DasGupta, C., & Radding, C. M. (1983) *Cell (Cambridge, Mass.) 34*, 931–939.

Bolivar, F., Rodriguez, R. L., Greene, P. J., Betlach, M. C., Heyneker, H. L., & Boyer, H. W. (1977) *Gene 2*, 95–113.

Brenner, S. L., Mitchell, R. S., Morrical, S. W., Neuendorf, S. K., Schutte, B. C., & Cox, M. M. (1987) *J. Biol. Chem. 262*, 4011–4016.

Christiansen, G., & Griffith, J. (1986) *Proc. Natl. Acad. Sci. U.S.A. 83*, 2066–2070.

Cox, M. M., & Lehman, I. R. (1981) *Proc. Natl. Acad. Sci. U.S.A. 78*, 3433–3437.

Cox, M. M., & Lehman, I. R. (1982) *J. Biol. Chem. 257*, 8523–8532.

Cox, M. M., & Lehman, I. R. (1987) *Annu. Rev. Biochem. 56*, 229–262.

Cox, M. M., McEntee, K., & Lehman, I. R. (1981) *J. Biol. Chem. 256*, 4676–4678.

Cox, M. M., Soltis, D. A., Livneh, Z., & Lehman, I. R. (1983) *J. Biol. Chem. 258*, 2577–2585.

Cox, M. M., Pugh, B. F., Schutte, B. C., Lindsley, J. E., Lee, J., & Morrical, S. W. (1987) in *DNA Replication and Recombination* (McMacken, R., & Kelly, T. J., Eds.) pp 597–607, Liss, New York.

Craig, N. L., & Roberts, J. W. (1981) *J. Biol. Chem. 256*, 8039–8044.

Cunningham, R. P., Wu, A. M., Shibata, T., DasGupta, C., & Radding, C. M. (1981) *Cell (Cambridge, Mass.) 24*, 213–223.

DasGupta, C., & Radding, C. M. (1982) *Proc. Natl. Acad. Sci. U.S.A. 79*, 762–766.

DasGupta, C., Shibata, T., Cunningham, R. P., & Radding, C. M. (1980) *Cell (Cambridge, Mass.) 22*, 437–446.

Davis, R. W., Botstein, D., & Roth, J. R. (1980) in *Advanced Bacterial Genetics*, pp 116–119, Cold Spring Harbor Laboratory, Cold Spring Harbor, NY.

Dretzen, G., Bellard, M., Sassone-Corsi, P., & Chambon, P. (1981) *Anal. Biochem. 112*, 295–298.

Dunn, K., Chrysogelos, S., & Griffith, J. (1982) *Cell (Cambridge, Mass.) 28*, 757–765.

Flory, J., & Radding, C. M. (1982) *Cell (Cambridge, Mass.) 28*, 747–756.

Flory, J., Tsang, S. S., & Muniyappa, K. (1984) *Proc. Natl. Acad. Sci. U.S.A. 81*, 7026–7030.

Howard-Flanders, P., West, S. C., & Stasiak, A. (1984) *Nature (London) 309*, 215–220.

Kaguni, J., LaVerne, L. S., & Ray, D. S. (1979) *Proc. Natl. Acad. Sci. U.S.A. 76*, 6250–6254.

Kahn, R., & Radding, C. M. (1984) *J. Biol. Chem. 259*, 7495–7503.

Kahn, R., Cunningham, R. P., DasGupta, C., & Radding, C. M. (1981) *Proc. Natl. Acad. Sci. U.S.A. 78*, 4786–4790.

Lohman, T. M., & Overman, L. B. (1985) *J. Biol. Chem. 260*, 3594–3603.

Lohman, T. M., Green, J. M., & Beyer, R. S. (1986) *Biochemistry 25*, 21–25.

Maniatas, T., Fritsch, E. F., & Sambrook, J. (1982) *Molecular Cloning: A Laboratory Manual*, pp 4–6, Cold Spring Harbor Laboratory, Cold Spring Harbor, NY.

McEntee, K., Weinstock, G. M., & Lehman, I. R. (1979) *Proc. Natl. Acad. Sci. U.S.A. 76*, 2615–2619.

Messing, J. (1983) *Methods Enzymol. 101*, 20–78.

Morrical, S. W., & Cox, M. M. (1987) *J. Biol. Chem.* (submitted for publication).

Morrical, S. W., Lee, J., & Cox, M. M. (1986) *Biochemistry 25*, 1482–1494.

Muniyappa, K., Shaner, S. L., Tsang, S. S., & Radding C. M. (1984) *Proc. Natl. Acad. Sci. U.S.A. 81*, 2757–2761.

Neuendorf, S. K., & Cox, M. M. (1986) *J. Biol. Chem. 261*, 8276–8282.

Pugh, B. F., & Cox, M. M. (1987a) *J. Biol. Chem. 262*, 1326–1336.

Pugh, B. F., & Cox, M. M. (1987b) *J. Biol. Chem. 262*, 1337–1343.

Radding, C. M., Flory, J., Wu, A., Kahn, R., DasGupta, C., Gonda, D., Bianchi, M., & Tsang, S. S. (1983) *Cold Spring Harbor Symp. Quant. Biol. 47*, 821–828.

Riddles, P. W., & Lehman, I. R. (1985) *J. Biol. Chem. 260*, 165–169.

Roman, L. J., & Kowalczykowski, S. C. (1986) *Biochemistry 25*, 7375–7385.

Shibata, T., Cunningham, R. P., DasGupta, C., & Radding, C. M. (1979) *Proc. Natl. Acad. Sci. U.S.A. 76*, 5100–5104.

Shibata, T., Cunningham, R. P., & Radding, C. M. (1981) *J. Biol. Chem. 256*, 7557–7564.

West, S. C., Cassuto, E., & Howard-Flanders, P. (1981) *Proc. Natl. Acad. Sci. U.S.A. 78*, 6149–6153.

Wu, A. M., Kahn, R., DasGupta, C., & Radding, C. M. (1982) *Cell (Cambridge, Mass.) 30*, 37–44.

Wu, A. M., Bianchi, M., DasGupta, C., & Radding, C. M. (1983) *Proc. Natl. Acad. Sci. U.S.A. 80*, 1256–1260.